RSC Advances

ROYAL SOCIETY OF CHEMISTRY

www.rsc.org/advances

Journal Name

COMMUNICATION

Preparation of SnO_2/graphene nanocomposite and its application to the catalytic epoxidation of alkenes with H_2O_2

Received 00th January 20xx,
Accepted 00th January 20xx

DOI: 10.1039/x0xx00000x

www.rsc.org/

Min Liu, Xiaozhong Wang, Yingqi Chen and Liyan Dai*

The in situ growth of SnO_2 nanoparticles on graphene has been obtained via a hydrothermal method and the nanocomposite was used as an efficient catalyst for the epoxidation of alkenes with aqueous hydrogen peroxide in nitrile based systems for the first time. Furthermore, the SnO_2/graphene nanocomposite could be readily recovered and reused for at least ten consecutive cycles without significant loss of the activity and selectivity.

Growing attention has been paid to the catalytic epoxidation of alkenes recently, since the obtained epoxides constitute highly valuable synthetic intermediates in the production of fine and bulk chemicals such as pesticides, pharmaceuticals, perfume and surfactant, etc.[1-5] Various heterogeneous catalysts containing transition metal have been employed for epoxidation, for instance, molybdenum-schiff base complexes supported on MCM-41 ,[6] Mg-Al layered double hydroxide (LDH),[7] immobilization of Mn^{2+} into zeolites[8] or a simple barium oxide[9]. However, multiple drawbacks such as low selectivity, bad oxidant efficiency, inevitable concomitant production and rapid loss of catalytic activity, still exist in these systems, which would hamper industrial application.

Another issue that concerns environmentalists is the use of undesirable oxidants, like peroxy acid, tert-butyl hydroperoxide and iodosylbenzene in conventional heterogeneous epoxidation reactions. Undoubtedly, dilute hydrogen peroxide is the ideal clean oxidant on environmental and economic grounds, owing to the outstanding advantages of low cost, non-toxicity, easy handling and the formation of water as the sole by-product.[10-12] Consequently, a sustainable epoxidation system should involve an effective catalyst that has higher metal capacity and activity in combination with green oxygen source. Recently we have noticed that basic solid catalysts show highly catalytic activity for epoxidation of alkenes using H_2O_2 in the presence of a nitrile, wherein nitrile acts as the activating agent to generate a peroxycarboximidic acid intermediate.[13-15]

Nowadays, graphene-based materials incorporated nanoparticles, such as noble metals (Pt,[16] Pd,[17] Au[18]), and transition-metal oxides (TiO_2,[19] Co_3O_4,[20] SnO_2,[21] WO_3,[22] NiO[23]) have been explored in many extending areas. Graphene possesses a high surface area for the good dispersion of metal or metal oxide,[17,20] two-dimensional structure for transfer of reactants and products, propitious electrical conductivity for electron transfer, which are attractive advantages in catalytic processes.[16-18,20] In addition, metal oxides like NiO[23] and Fe_2O_3[24] could anchor strongly on the graphene through covalent bond interactions.

Intrigued by these appealing properties of graphene，we first reported here the graphene incorporated SnO_2 as an efficient and recyclable catalyst for epoxidation, which was synthesized via a facile in situ hydrothermal strategy by oxidizing $SnCl_2$ with graphene oxide (GO).[25] Graphite oxide, the precursor of graphene, was synthesized according to a modified Hummer method from graphite powder.[26] Given that graphite is relatively inexpensive, achieving graphene sheets on a large scale is strongly desirable. The obtained SnO_2/reduced graphene oxide (SnO_2/RGO) nanocomposite exhibited superior catalytic activitiy and impressively good reusability for the epoxidation with H_2O_2 (30 wt%) in nitrile based system, wherein the active species leached little without obvious aggregation.

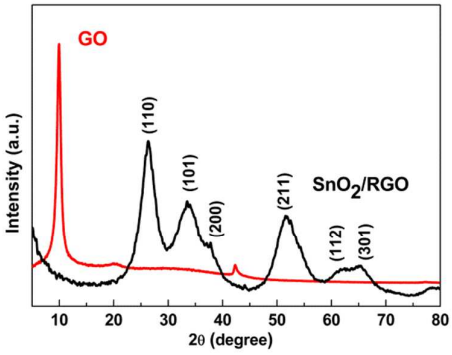

Fig. 1 XRD patterns of GO and SnO_2/RGO nanocomposite

College of Chemical and Biological Engineering, Zhejiang University, Hangzhou, P.R.China. E-mail: dailiyan@zju.edu.cn; Fax: +86-571-87952693; Tel: +86-571-87952693

Electronic Supplementary Information (ESI) available: [details of any supplementary information available should be included here]. See DOI: 10.1039/x0xx00000x

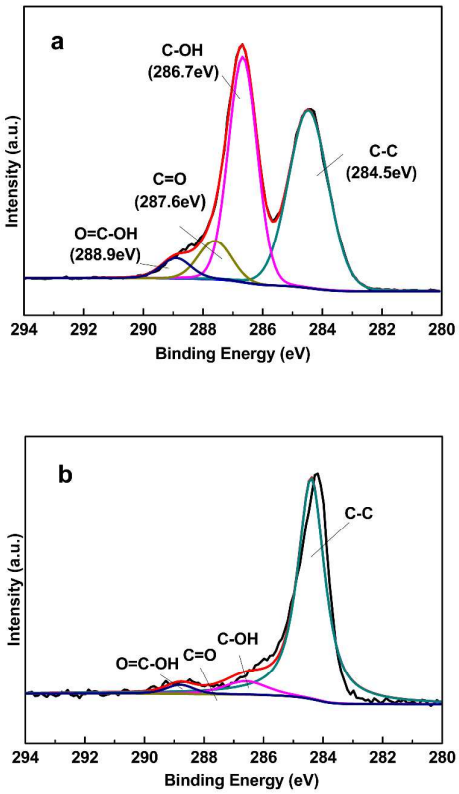

Fig. 2 XPS spectra of (a) C 1s of GO; (b) C 1s of SnO_2/RGO.

The XRD patterns of graphene oxide and SnO_2/RGO nanocomposite are illustrated in the Fig. 1. A sharp and strong peak at 10.0° in curve provided evidence for the formation of GO.[27] The five dominant broadened peaks at 26.6°, 33.8°, 51.7°, 64.7° and 65.9° in pattern of SnO_2/RGO correspond to (110), (101), (211), (112) and (301) of SnO_2 (PDF No. 41-1445) , respectively, unambiguously demonstrating the formation of tetragonal rutile SnO_2 nanocrystals. However, no obvious diffraction peaks assigned to RGOs were found in the XRD pattern of the SnO_2/RGO composite, probably because the amount of graphene sheets in SnO_2/RGO was very low, which was confirmed by the TG curve (Fig. S1, ESI).

The XPS spectrum of the composite in Fig. S2a obviously suggested the presence of carbon, oxygen and tin. The Sn $3d_{5/2}$ (486.9eV) and Sn $3d_{3/2}$ (495.5eV) with an 8.6 eV peak-to-peak separation in Fig. S2b further confirmed the formation of SnO_2 nanoparticles.[27] The C 1s XPS spectra of GO and SnO_2/RGO nanocomposite are shown in Fig. 2a and Fig. 2b, respectively. This region can be fitted into four peaks: nonoxygenated ring C (C–C, C=C and C–H) at 284.5 eV, carbon in C–OH at 286.7 eV, carbonyl carbon (C=O) at 287.6 eV and C=O–OH species at 288.9 eV. Compared to graphene oxide, the intensity of these oxygenated functional groups in SnO_2/RGO decreases significantly, indicating that graphene oxide was deoxygenated to graphene by Sn^{2+} ion partly[28] besides hydrothermal procedure.

FTIR spectra of the obtained samples are shown in Fig. S3. Compared to pure stannic oxide, a strong peak at 584 cm^{-1} is associated to Sn-O, clarifying that SnO_2 particles exist.[28] In the case of SnO_2/RGO, the peaks assigned to carboxyl (1732 cm^{-1}) and epoxy (1066 cm^{-1}) functional groups are even absent, which also indicates the successful reduction of graphene oxide and the formation of SnO_2/RGO.

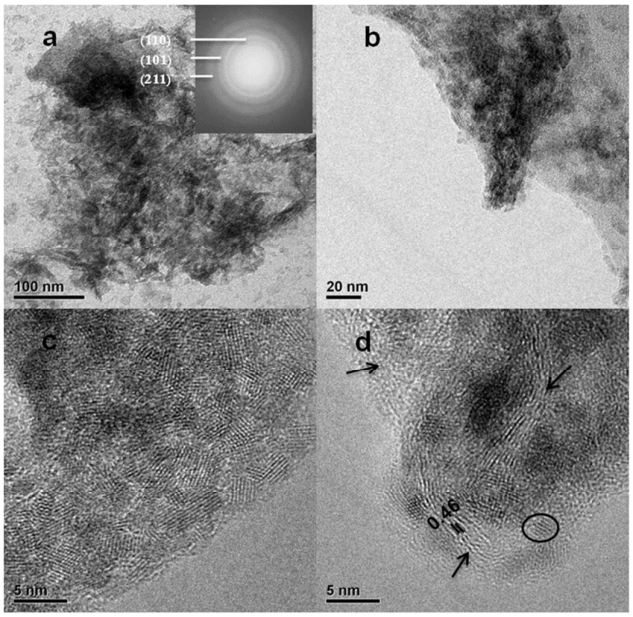

Fig. 3 (a) Low magnification TEM image of SnO_2/RGO composite and the corresponding selected area electron diffraction (SAED); (b) high magnification TEM image of SnO_2/RGO composite; (c) HRTEM image of SnO_2/RGO composite; (d) HRTEM image of an edge-side of the SnO_2/RGO composite.

From the representative TEM images of the composite (Fig. 3a and 3b), it is evident that a large amount of SnO_2 nanoparticles are uniformly deposited on the two-dimensional graphene sheets with high density. The HRTEM image in Fig. 3c demonstrates that the grain size of SnO_2 nanoparticles can be determined to be around 3 nm. The HRTEM image of the SnO_2/RGO taken from an edge (Fig. 3d) exhibits that the layer numbers of the stacked graphene nanosheets in this composite are mainly in the range from three to six. It indicates that the in situ growth of SnO_2 on RGOs not only prevented the aggregation of SnO_2 nanopaticles, but also preserved the 2-dimensional structure of graphene nanosheets.

To evaluate the catalytic efficiency of the SnO_2/RGO nanocomposite, the epoxidation of cyclohexene with 30 wt% H_2O_2 in the $NaHCO_3$ buffer system was carried out, and the results are presented in Table 1. Interestingly, the conversion and selectivity were moderate in the blank experiment (entry 1). Various metal oxides were also examined for comparison purposes. Among these screened metal oxides, only SnO_2 displayed superior activity over the other catalysts both in conversion and selectivity. However, the SnO_2 nanoparticles are easy to aggregate, and thus it is essential to find a suitable template to minimize the aggregation problem. Notably, SnO_2/RGO nanocomposite was more efficient compared to other supported SnO_2 catalysts, suggesting the superiority of the graphene support (entries 10 and 11 vs. entry 13). Obviously, $SnCl_2 \cdot 2H_2O$, GO and RGO didn't promote the reaction (entries 7, 8 and 9). SnO_2/RGO exhibited the highest epoxide selectivity of up to 98.2% with a conversion of 92.5% when the catalyst amount was 5

mol%, which illustrated that SnO_2/RGO nanocomposite is an excellent heterogeneous catalyst for this reaction. We believe that the unique two-dimensional structure properties of graphene were responsible for the enhanced catalytic performance, which not only provided good dispersion of metal oxide but also facilitated accessibility to the catalytic sites on the nanocomposite surfaces for the reactants. Beyond that, the in situ growth of SnO_2 on RGOs reduced the aggregation problems mutually, which preferred to increase accessible reaction sites compared with single SnO_2. The oxidation hardly occurred without acetonitrile (see Table S1), which suggested that the presence of acetonitrile is essential to perform the reaction, which was similar to Payne epoxidation.[29,30] As to traditional hydrotalcite catalysis in related systems, the basic hydroxy groups of the hydrotalcites could substitute for the buffer solution but undesirable solvent such as methanol should be added.[31,32]

Table 1 Epoxidation of cyclohexene catalyzed by SnO_2/RGO and other catalysts[a]

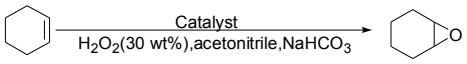

Entry	Catalyst	Catalyst amount[b] (mol% of cyclohexene)	Conversion[c] (%)	Epoxide selectivity (%)[d]
1	blank	-	67.6	86.3
2	WO_3	5	77.1	79.4
3	MgO	5	85.7	68.8
4	TiO_2	5	57.5	28.3
5	ZnO	5	66.7	60.1
6	SnO_2	5	80.5	90.3
7	GO[e]	-	66.7	5.3
8	$SnCl_2{\cdot}2H_2O$	5	20.7	3.9
9	RGO[e]	-	51.5	86.8
10	SnO_2/Graphite[f]	5	75.1	84.6
11	SnO_2/SiO_2[f]	5	85.9	91.3
12	SnO_2/RGO	2.5	90.9	89.7
13	SnO_2/RGO	5	92.5	98.2
14	SnO_2/RGO	7.5	92.9	97.5
15	SnO_2/RGO	10	90.4	89.1

a Reaction conditions: cyclohexene (10 mmol), acetonitrile (5 mL), $NaHCO_3$ (0.2M, 5mL), H_2O_2 (30 wt%, 12mmol), 50 °C, 3 h. *b* Catalyst amount is the mol% of cyclohexene regarding catalytic active species. *c* Conversion and selectivity were determined by GC and identified by GC-MS. *d* Main by-products : cyclohexenol, cyclohexenone and others. *e* Catalyst 100mg. *f* Catalyst 190mg(5 mol% of cyclohexene regarding catalytic SnO_2 sites).

The effect of the catalyst amount on the catalytic performance was also examined. The lower selectivity was observed when the catalyst amount was reduced to 2.5 mol%. With the increase in the catalyst amount, the cyclohexene oxide conversion rose slightly, whereas a further addition of catalyst (10 mol%) decreased the epoxide selectivity from 97.5% to 89.1%. A higher catalyst amount causing lower performance might result from redundant active sites leading to the decomposition of the oxidant.[33] So it could be concluded that only with a suitable amount of catalyst the catalytic performance was prone to be the best for the present reaction system. The influence of other factors has also been discussed, which showed that modestly elevated temperatures were required to obtain a significant increase in catalytic performance and 1.2 molar equivalents H_2O_2 per mole of the substrate were appropriate (see Table S1).

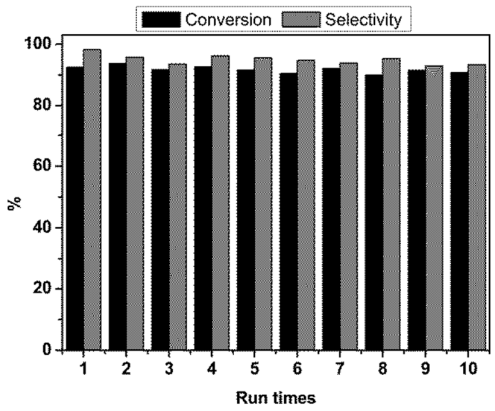

Fig. 4 Reusability of SnO_2/RGO in the epoxidation of cyclohexene. Reaction conditions: cyclohexene (10 mmol), acetonitrile (5 mL), $NaHCO_3$ (0.2M, 5mL), H_2O_2 (30 wt%, 12mmol), 50 °C, 3 h.

Table 2 Epoxidation of various alkenes catalyzed by SnO_2/RGO nanocomposite[a]

Entry	Substrate	Product	Conversion[b] (%)	Selectivity (%)
1		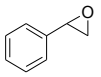	93.4	81.4
2	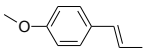	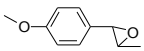	86.2	57.8
3			92.5	98.2
4			98.8	99.0
5			>99	67.6
6			30.5	100
7	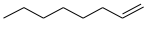	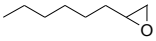	41.3	100

a Reaction conditions: substrate (10 mmol), SnO_2/RGO nanocomposite (100mg, 5 mol% of substrate), acetonitrile (5 mL), $NaHCO_3$ (0.2M, 5mL), H_2O_2 (30 wt%, 12mmol), 50 °C, 3 h. *b* Conversion and selectivity were determined by GC and identified by GC-MS.

Another advantage of the SnO_2/RGO nanocomposite is the robust reusability, which is a prerequisite for practical applications. After the reaction, the solid catalyst was separated from the reaction mixture conveniently by simple filtration. The recyclability was then tested under the identical conditions through the epoxidation of cyclohexene. The results in Fig. 4 demonstrated that the heterogeneous catalyst was fairly stable for ten cycles without observing significant decrease in catalytic activity. Both conversion and selectivity were still higher than 90% throughout ten runs. The robust recyclability of SnO_2/RGO nanocomposite may originate from the strong interactions between graphene and metal oxide.

Evidence for the stability of our catalyst can be seen in further tests. The XRD patterns of the fresh and the reused one (after 10 recycles) are shown in Fig. S6. Obviously, there is no discriminable difference between the fresh catalyst and the spent one, indicating that the characteristic peaks of tetragonal SnO_2 still exist. The TEM image of the recovered catalyst (Fig. S7) further confirmed that the size of SnO_2 is still around 3nm intuitively after ten recycles, suggesting that graphene prevent the aggregation problem efficiently. The result of ICP-AES analysis showed no trace of Sn in the filtrate, which is also confirmed by the TG curves (Fig. S8), as the amount of active spieces remained at 77% in consecutive cycles. These results infer that the nanocomposite is truly heterogeneous with no active spieces leaching.

Furthermore, the generality of this catalytic system was then investigated under the optimized reaction conditions. As shown in Table 2, styrene showed a conversion of 93.4% and selectivity of 81.4% (entry 1) and the epoxidation was also successfully carried out on norbornene (entry 4). Anethole and allyl alcohol showed relatively high conversion with lower selectivity (entries 2 and 5). The conversion of isophorone and 1-octene were significantly lower than other alkenes (entries 6 and 7), which possibly because weaker electrophilic cycloaddition would occur in the epoxidation of electron-deficient alkenes.

Conclusions

In conclusion, we have demonstrated for the first time that SnO_2/RGO nanocomposite can be used as an excellent catalyst in the epoxidation of alkenes with a combined oxidant of H_2O_2 (30 wt%) and acetonitrile. The catalyst is recyclable and stable, which can be reused for at least ten times with no appreciable loss in its catalytic activity. Furthermore, the XRD and TEM analyses of the reused catalyst disclosed that the nanoparticles still dispersed homogeneously on graphene sheets without any aggregation, indicating the unique layered structure of graphene minimized the aggregation problem effectively. Additionally, the use of H_2O_2 with only 1.2 molar equivalents is another attractive advantage. Other chemical reactions in this catalytic system are under investigation in our laboratory.

Acknowledgements

This work was supported by the NSFC (No: 21176213), and Zhejiang Key Innovation Team of Green Pharmaceutical Technology (No: 2010R50043).

Notes and references

1 Q. H. Xia, H. Q. Ge, C. P. Ye, Z. M. Liu and K. X. Su, *Chem. Rev.*, 2005, **105**, 1603-1662.
2 P. J. Cordeiro and T. D. Tilley, *ACS Catal.*, 2011, **1**, 455-467.
3 L. Wang, H. Wang, P. Hapala, L. Zhu, L. Ren, X. Meng, J. P. Lewis and F. S. Xiao, *J. Catal.,* 2011, **281**, 30-39.
4 S. A. Hauser, M. Cokoja and F. E. Kühn, *Catal. Sci. Technol.*, 2013, **3**, 552-561.
5 D. Banerjee, R. V. Jagadeesh, K. Junge, M. M. Pohl, J. Radnik, A. Brückner and M. Beller, *Angew. Chem. Int. Ed.*, 2014, **53**, 4359-4363.
6 M. Masteri-Farahani, F. Farzaneh and M. Ghandi, *J. Mol. Catal. A: Chem.*, 2006, **248**, 53-60.
7 E. Angelescu, O. Pavel, R. Bîrjega, M. Florea and R. Zăvoianu, *Appl. Catal. A*, 2008, **341**, 50-57.
8 B. Qi, X. H. Lu, D. Zhou, Q. H. Xia, Z. R. Tang, S. Y. Fang, T. Pang and Y. L. Dong, *J. Mol. Catal. A: Chem.,* 2010, **322**, 73-79.
9 V. R. Choudhary, R. Jha and P. Jana, *Green Chem.*, 2006, **8**, 689-690.
10 K. Kamata, K. Yonehara, Y. Sumida, K. Yamaguchi, S. Hikichi and N. Mizuno, *Science*, 2003, **300**, 964-966.
11 G. Grigoropoulou, J. Clark and J. Elings, *Green Chem.,* 2003, **5**, 1-7.
12 A. Russo, C. De Fusco and A. Lattanzi, *ChemCatChem*, 2012, **4**, 901-916.
13 K. Yamaguchi, K. Ebitani and K. Kaneda, *J. Org. Chem.*, 1999, **64**, 2966-2968.
14 U. R. Pillai, E. Sahle-Demessie and R. S. Varma, *Tetrahedron Lett.*, 2002, **43**, 2909-2911.
15 M. Romero, J. Calles, M. Ocana and J. Gomez, *Microporous Mesoporous Mater.*, 2008, **111**, 243-253.
16 E. Yoo, T. Okata, T. Akita, M. Kohyama, J. Nakamura and I. Honma, *Nano Lett.*, 2009, **9**, 2255-2259.
17 X. Chen, G. Wu, J. Chen, X. Chen, Z. Xie and X. Wang, *J. Am. Chem. Soc.*, 2011, **133**, 3693-3695.
18 J. Li, C. y. Liu and Y. Liu, *J. Mater. Chem.*, 2012, **22**, 8426-8430.
19 G. Williams, B. Seger and P. V. Kamat, *ACS nano*, 2008, **2**, 1487-1491.
20 R. Nie, J. Shi, W. Du, W. Ning, Z. Hou and F. S. Xiao, *J. Mater. Chem. A*, 2013, **1**, 9037-9045.
21 S. M. Paek, E. Yoo and I. Honma, *Nano Lett.*, 2008, **9**, 72-75.
22 B. Weng, J. Wu, N. Zhang and Y. J. Xu, *Langmuir*, 2014.
23 G. Zhou, D. W. Wang, L. C. Yin, N. Li, F. Li and H. M. Cheng, *Acs Nano*, 2012, **6**, 3214-3223.
24 B. Sun, Z. Jiang, D. Fang, K. Xu, Y. Pei, S. Yan, M. Qiao, K. Fan and B. Zong, *ChemCatChem*, 2013, **5**, 714-719.
25 H. Song, L. Zhang, C. He, Y. Qu, Y. Tian and Y. Lv, *J. Mater. Chem.*, 2011, **21**, 5972-5977.
26 S. Gilje, S. Han, M. Wang, K. L. Wang and R. B. Kaner, *Nano Lett.*, 2007, **7**, 3394-3398.
27 Y. Wang, I. Djerdj, B. Smarsly and M. Antonietti, *Chem. Mater.*, 2009, **21**, 3202-3209.
28 Y. Li, X. Lv, J. Lu and J. Li, *J. Phys. Chem. C*, 2010, **114**, 21770-21774.
29 G. B. Payne, P. H. DEMING and P. H. WILLIAMS, *J. Org. Chem.*, 1961, **26**, 659-663.
30 W. C. Frank, *Tetrahedron: Asymmetry*, 1998, **9**, 3745-3749.
31 S. Ueno, K. Yoshida, K. Ebitani and K. Kaneda, *Chem. Commun.*, 1998, 295-296.
32 I. Kirm, F. Medina, X. Rodríguez, Y. Cesteros, P. Salagre and J. Sueiras, *Appl. Catal., A*, 2004, **272**, 175-185.
33 W. Zheng, R. Tan, L. Zhao, Y. Chen, C. Xiong and D. Yin, *RSC Adv.*, 2014, **4**, 11732-11739.

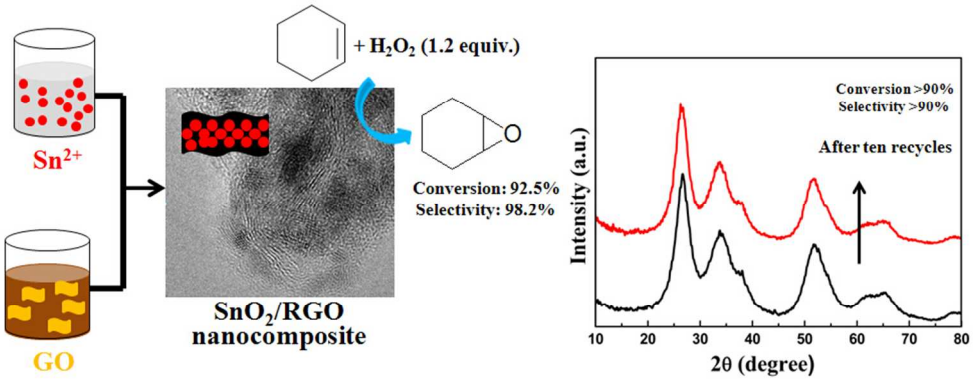

263x107mm (96 x 96 DPI)